

Supporting Information

Experimental and Theoretical Investigation of a Stable Zinc-Based Metal-Organic Framework for CO₂ Removal from Syngas

Ruiqin Zhong,^{*,a} Jia Liu,^b Xing Huang,^a Xiaofeng Yu,^a Changyu Sun,^a Guangjin Chen,^a and Ruqiang Zou^{*,b}

a State Key Laboratory of Heavy Oil Processing, China University of Petroleum, Beijing 102249, China

b College of Engineering, Peking University, Beijing 100871, China.

1. Synthesis of organic ligand

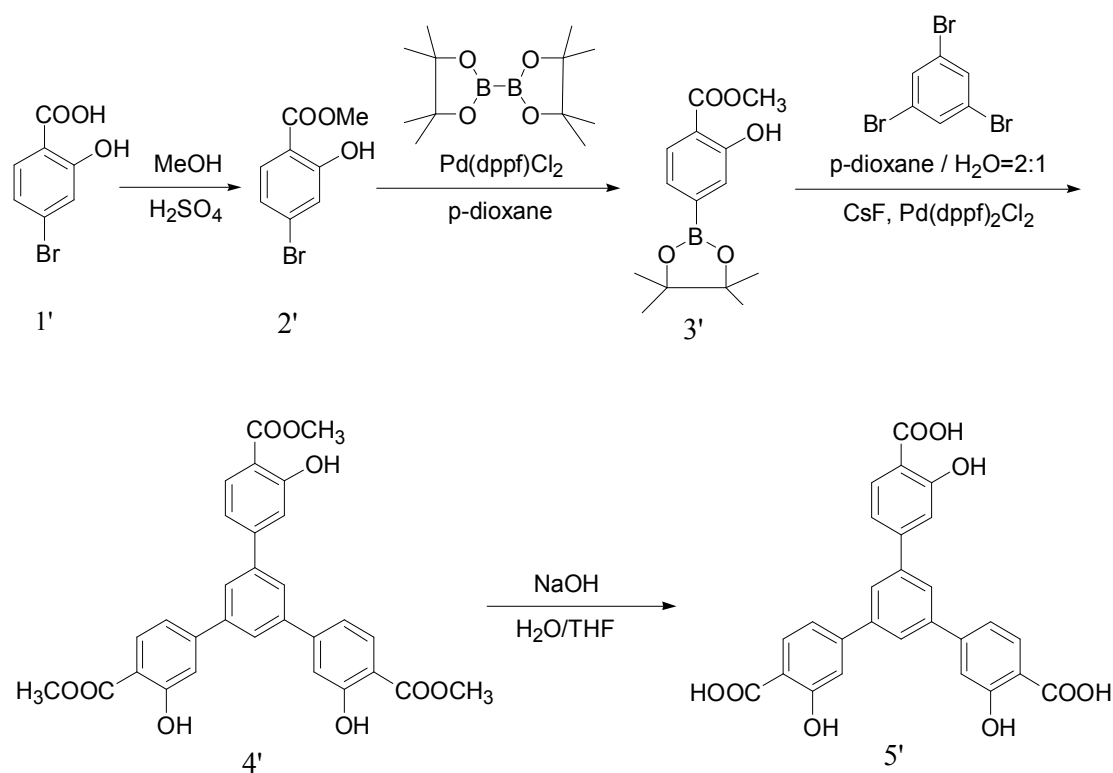
1.1 Materials and General Methods.

All the starting reagents and solvents for synthesis were commercially available and used without further purification.

^1H and $^{13}\text{C}\{^1\text{H}\}$ NMR spectra were acquired on a Bruker ARX-500 (500 MHz), DRX-500 (500 MHz) spectrometer at 297–300 K, and chemical shifts were calculated using the solvent resonances as internal standards (^1H : 2.50 ppm for DMSO; $^{13}\text{C}\{^1\text{H}\}$: 39.51 ppm for DMSO-*d*6). Column chromatography was performed on silica gel purchased from Sorbent Technologies (standard grade, 60 Å, 40–63 m).

1.2 Procedures and spectral data

Synthesis of the ligand (**5'**) was started with 4-bromo-2-hydroxybenzoic acid (**1'**) and followed the reaction routes shown below.



Scheme S1. Synthetic scheme of 1,3,5-tri(3-hydroxy-4-carboxyl)phenylbenzene (**5'**).

Methyl 4-bromo-2-hydroxybenzoate (2').

A solution of 4-bromo-2-hydroxybenzoic acid (**1'**) (23.8 g) in MeOH (300 mL) was treated with concentrate sulfuric acid (8 mL). The mixture was refluxed for 10 h, poured onto ice-water, and extracted with CH₂Cl₂. The combined organics were washed with saturated aqueous NaHCO₃, dried over Na₂SO₄, and concentrated to give the ester.

Methyl 2-hydroxy-4-(4, 4, 5, 5-tetramethyl-1, 3, 2-dioxaborolan-2-yl) benzoate (3').

Anhydrous *p*-dioxane (350 mL) was added to a round bottom flask charged with methyl 4-bromo-2-hydroxybenzoate (22.3 g), bis(pinacolato)diboron (40.6 g), KOAc (23.5 g) and Pd(dppf)Cl₂(0.49 g). The reaction mixture was heated at 85 °C for 18 h under N₂ atmosphere, before being cooled to room temperature and filtered subsequently to remove insoluble salts which were washed further with EtOAc. The filtrate was concentrated in vacuo before re-dissolving the residue in EtOAc. Ample activated carbon was added to the typically dark brown/black solution and the EtOAc solution was warmed to reflux for 15 min. The insoluble material was removed by hot filtration to provide typically a yellow solution that was concentrated in vacuo to provide an oil. The product was used for the next step without further purification.

1,3,5-tri(3-hydroxyl-4-methoxycarbonyl)phenylbenzene (4').

Methyl 2-hydroxy-4-(4, 4, 5, 5-tetramethyl-1, 3, 2-dioxaborolan-2-yl) benzoate (4.67 g), 1,3,5-tribromobenzene(6.26 g), CsF (5.1 g) and Pd(dppf)₂Cl₂ (0.1 g) were dissolved in a *p*-dioxane/H₂O (200 mL, 2:1 v/v) mixture, then, the resulting mixture was heated at 90 °C under N₂ atmosphere and stirred vigorously until completion of the reaction (progress periodically checked by TLC). After cooled down to room temperature, the reaction mixture was quenched by water and extracted with CH₂Cl₂ (2 × 100 mL). The organic layers were combined, dried over Na₂SO₄, filtered, and

evaporated in vacuo to provide a solid. The product was purified by column chromatography.

^1H NMR (500 MHz, $\text{DMSO-}d_6$), [ppm]: 10.81(s, 3H), 7.90(d, 3H), 7.80(s, 3H), 7.26(d, 3H), 7.16-7.17(q, 3H), 3.98(s, 9H).

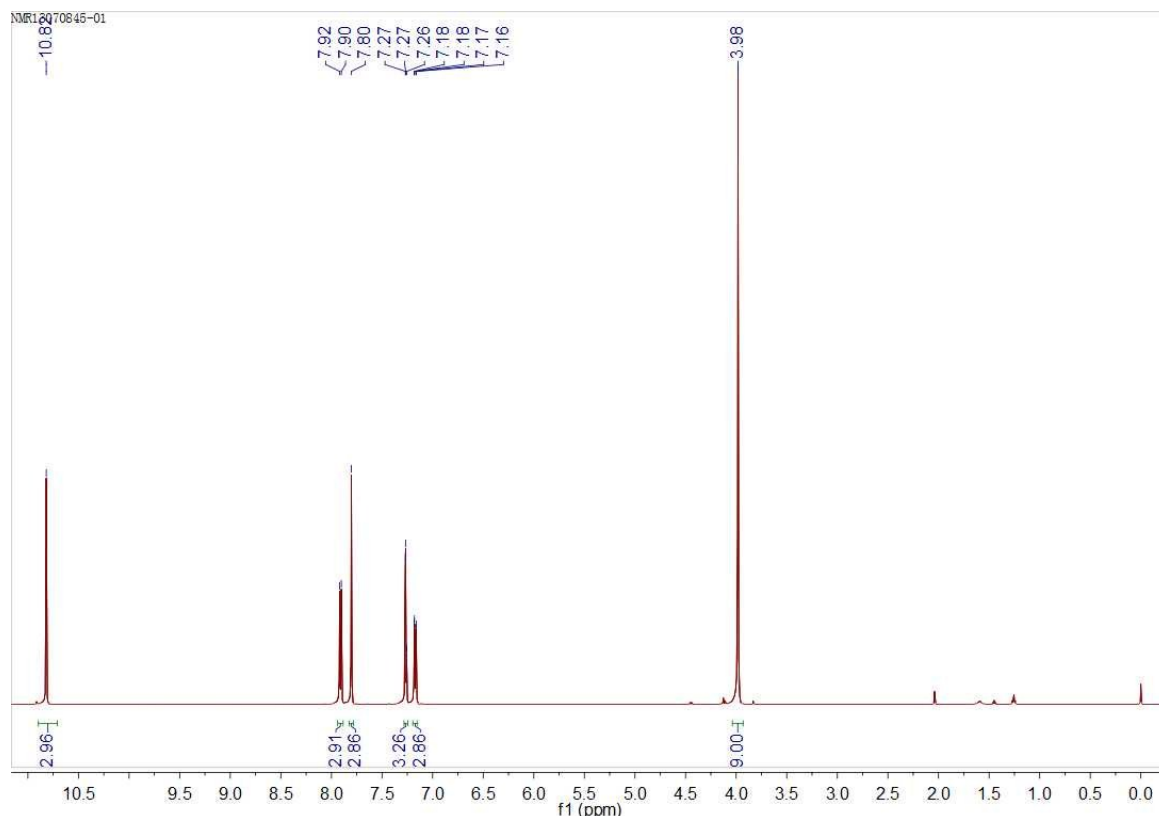


Figure S1. ^1H NMR spectra of **4'** in $\text{DMSO-}d_6$.

1,3,5-tri(3-hydroxyl-4-carboxyl)phenylbenzene (5').

To a solution of dimethyl 3,3''-dihydroxy-5'-(3-hydroxy-4-(methoxycarbonyl)phenyl)-[1,1':3',1''-terphenyl]-4,4''-dicarboxylate (2.43 g) in THF (100 mL) was added a solution of NaOH (2.0 g) in H_2O (100 mL). The resulting solution was stirred vigorously at 50°C until the reaction completes (progress periodically checked by TLC). After cooled down to room temperature, the aqueous was acidified with concentrate HCl while being stirred and the resulting precipitate

was collected by vacuum filtration, washed with ample H₂O, and dried in air for 24 h then in vacuo for 6 h to provide the corresponding hydrolysed product as typically a white powder.

¹H NMR (500 MHz, DMSO-*d*₆), [ppm]: 8.03(3, 3H), 7.90(t, 3H), 7.53(q, 3H), 7.46-7.48(m, 3H). ¹³C{¹H} NMR (125 MHz, DMSO-*d*₆), [ppm]: 171.75, 161.51, 146.56, 140.31, 130.72, 125.76, 118.25, 115.48, 112.26.

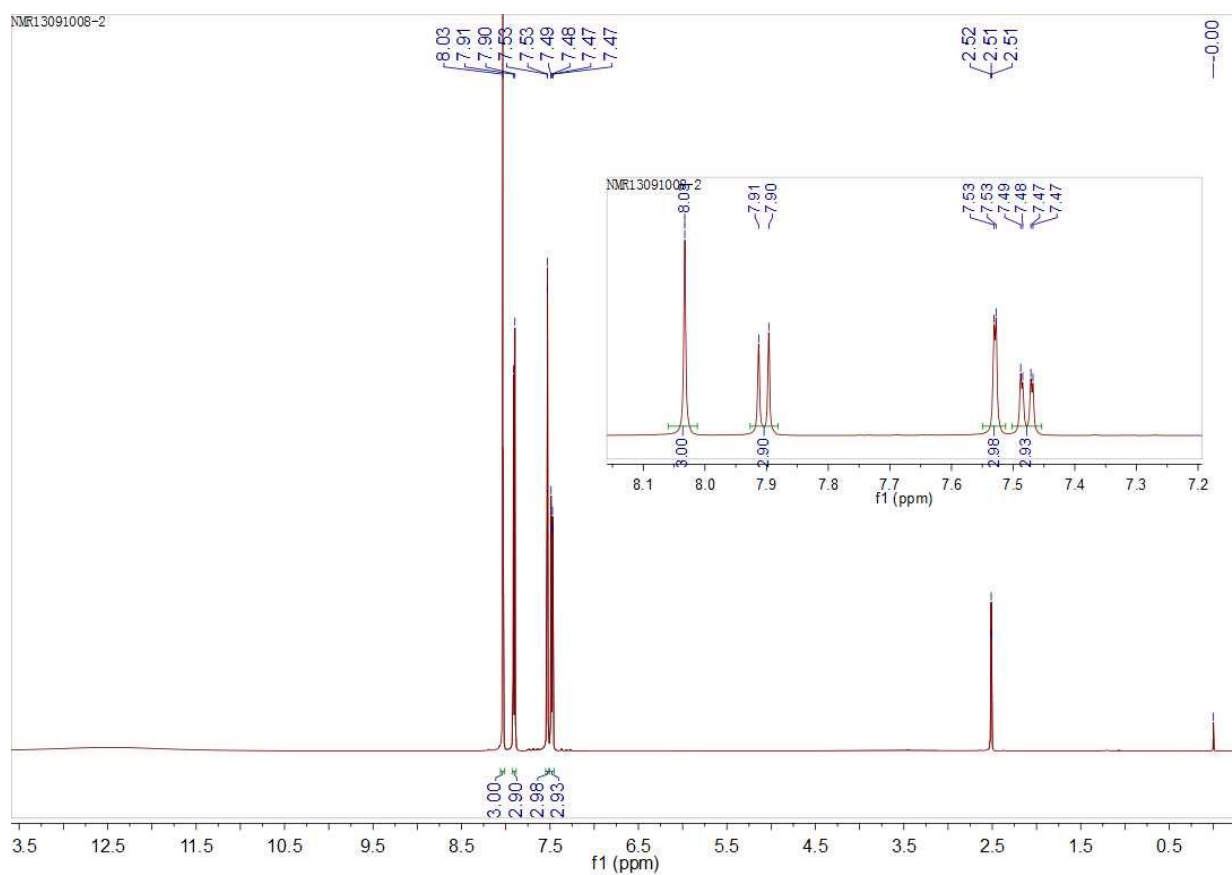


Figure S2. ¹H NMR spectra of **5'** in DMSO-*d*₆. Inset, expanded aromatic region in the spectra.

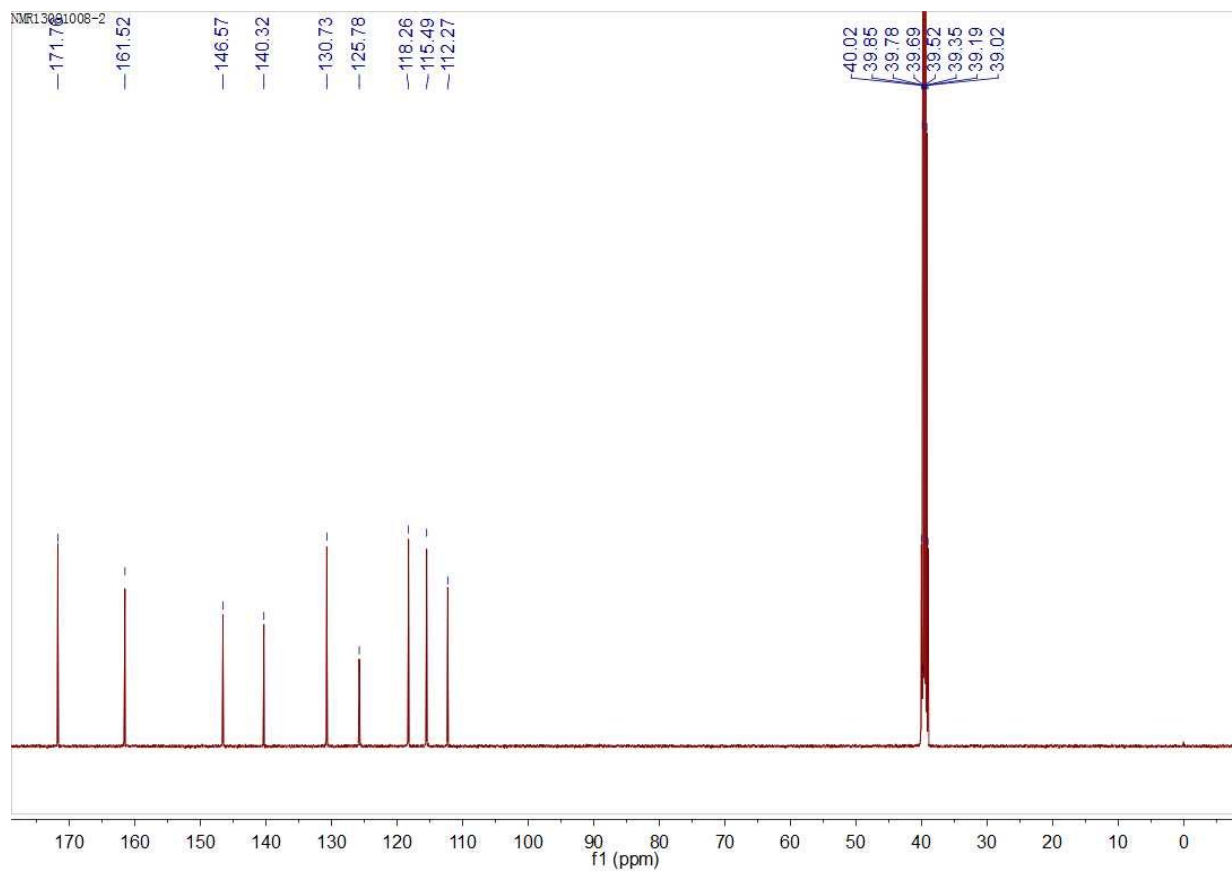


Figure S3. $^{13}\text{C}\{^1\text{H}\}$ NMR spectra of **5'** in $\text{DMSO-}d_6$.

2. Material Characterization

Fourier Transform Infrared spectroscopy (FT-IR) was recorded using an ECTOR22 Fourier transform infrared spectrometer between 400 cm⁻¹ and 4000 cm⁻¹ in KBr pellets. Powder X-ray diffraction (PXRD) was performed on a Rigaku Dmax/2400 X-ray diffractometer operating at 40 kV and 100 mA, using Cu-K α radiation ($\lambda=1.5406 \text{ \AA}$). Thermo gravimetric analysis (TGA) was carried out under nitrogen atmosphere on a Q600 SDT TGA-DTA-DSC thermal analyzer from room temperature to 700 °C with a heating rate of 10 °C min⁻¹.

3. Gas Sorption Measurements

Ultra-high purity grade N₂ (99.999%), He (99.999%), H₂ (99.999%), CO₂ (99.999%) and CO (99.999%) were used for all adsorption measurements.

Gas adsorption measurements were carried out with QUANTACHROME AUTOSORB-iQ gas adsorption analyzer. The N₂ sorption isotherms were collected in the pressure range from 0.01 to 0.99 P/P₀ at 77K in a liquid nitrogen bath. CO₂, CO and H₂ adsorption isotherms were collected in the pressure range from 0.01 to 0.99 P/P₀ at 273K in a circulator with temperature controller with a mixture of 50 v % water and 50 v % ethylene glycol.

The isosteric heat was calculated from isotherm curve at different temperature according to the Clapeyron equation.

The selectivities of CO₂/CO and CO₂/H₂ for **1** were calculated from the Henry constants. Dual-site Langmuir isotherms [Eq (1)] were employed to analyze the CO₂ adsorption isotherm.

$$V(\text{CO}_2) = \frac{V_1 K_1 P}{1 + K_1 P} + \frac{V_2 K_2 P}{1 + K_2 P} \quad (1)$$

$V(\text{CO}_2)$ represents the whole volume of CO₂ that absorbed; V_1 and V_2 , the CO₂ capacity that absorbed for the contributions of the dual site Langmuir Isotherm; K_1 and K_2 , the constant of CO₂ adsorption that adsorbed for the contributions of the dual site Langmuir Isotherm. P , the applied pressure.

The CO and H₂ adsorption isotherms were calculated by replacing to single

Langmuir isotherms [Eq (2)].

$$V = \frac{V_1 K_1 P}{1 + K_1 P} \quad (2)$$

V_1 , the CO₂ capacity that adsorbed; K_1 , constants corresponding to the calculation;

According to IAST adsorbed gas can be treated as two dimension phase. Chemical potential of each component in adsorptive phase must be equal to it in gas phase. Ignoring the intermolecular force between adsorbates the relationship of one component in two phases should be following Raoult's law when a system reach equilibrium:

$$P y_i = P_i^0(\pi) x_i \quad (3)$$

P_i^0 is pressure of pure component i when it lead to the same surface tension in adsorbed phase. x_i is mole fraction of component i in adsorptive phase. y_i is mole fraction of component i in gas phase, P is the pressure of gas phase.

According to Gibbs equation, the following equation was established.

$$\frac{\pi A}{RT} = \int_0^{P_i^0} \frac{n}{P} dP \quad (4)$$

In equilibrium each surface tension of component in adsorptive phase should be equal, sum of the mole fraction of each component should be 1

$$\int_0^{P_i^0} \frac{n_i}{P} dP = \int_0^{P_j^0} \frac{n_j}{P} dP \quad (i,j=1,\dots,m) \quad (5)$$

$$\sum_{i=1}^4 x_i = 1$$

(6)

Importing isotherm equation into the equation (4) (5) (6) the relationship of pressure and uptakes of each component should be obtained which can be used to calculate selectivity.

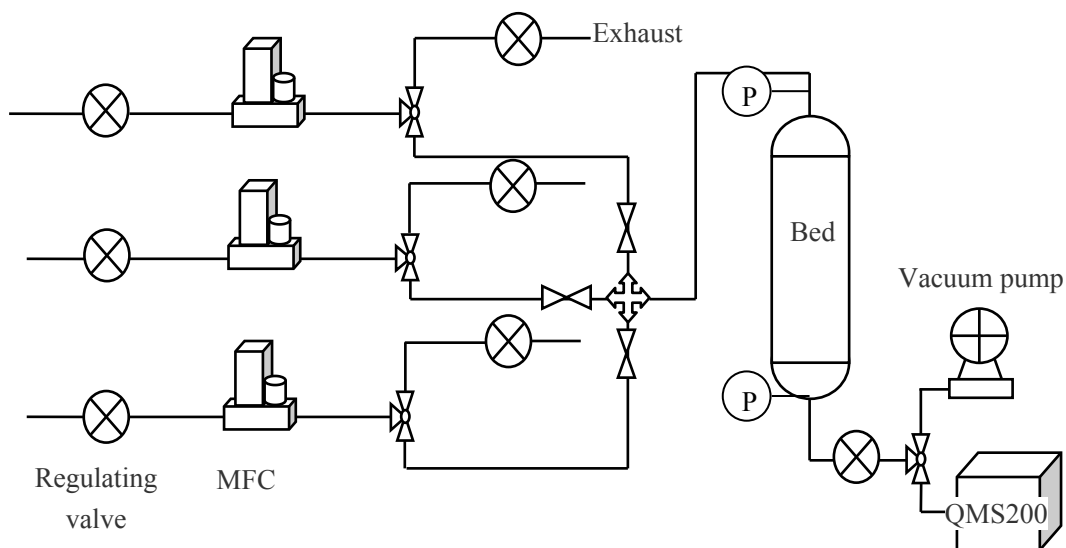
$$Selectivity = \frac{(x/y)_i}{(x/y)_j} \quad (7)$$

4. MC simulation

The models of sample 1 were used for simulation. The unit cells of frameworks adopted in this simulation were $2 \times 2 \times 2$ with periodic boundary. The frameworks were treated as rigid with frozen atoms during simulation. A total of 2×10^7 steps were used; the first half moves were used for equilibration, and the remaining steps were used for calculating the ensemble averages. The potential parameter values for frameworks and gas molecules were from the COMPASS force field. The adsorption of CO_2 , CO and H_2 were calculated using Monte Carlo (MC) simulations in the grand canonical ensemble.

5. Breakthrough Measurements

Gas breakthrough experiments were performed with a mixture of CO_2 (19.96 v%) and syngas (10.02 v% CO and 35.04 v% H_2), diluted by helium (34.98 v%). Experiments were carried out at 273 K, and 0.1 MPa and 1 MPa respectively. The breakthrough experiments apparatus were a homemade setup shown schematically in Fig S4.



FigureS4. Schematic of breakthrough experiment

The adsorbents were packed in a stainless steel tube of length 80mm and inner diameter 4mm. Mass flow controllers of precision $\pm 1\%$ (purchased from Beijing seven star electronics Co LTD) were used to control the flow rates in the passages of the absorber: A back-pressure regulator was used to control the pressure over the

adsorption bed and a pressure transducer with accuracy $\pm 0.1\%$ was used to detect the pressure. Pressure at both entrance and exit of the adsorption bed was detected, and the pressure drop over the bed was thus obtained. Composition of exhausted gas was analyzed by a QMS 200 type Quadra-pole mass spectrograph manufactured by the USA. All parts were connected with stainless steel capillary tubes of inner diameter 2mm and wall thickness 0.5mm. The computer recorded the variation of signals with time and issued commands.

The pre-activated sample was heated in situ at 100 °C for 5 hours in flowing Helium to remove residual water absorbed during sample loading, which requires brief exposure to ambient air.

The gas selectivity was evaluated on the basis of equilibrium adsorbed amount calculated from breakthrough curves. The breakthrough curves record the variation of concentration with time. When all components have broken through and reached the equilibrium, the follow equation exists on the basis of mass balance:

$$\int_0^t q_{in} C_{i,in} dt = \int_0^t q_{out} C_{i,e} dt + V_{\epsilon} C_{i,in} P / RT + W_i n_i \quad (8)$$

| | | | |
|------|--------------------------------|-------------------|--|
| c | concentration of components, % | q | flow rate, ml/min |
| n | amount adsorbed, mmol/g | V | specific pore volume, cm ³ /g |
| P | pressure, MPa | W | Weight of adsorbents ,g |
| R | gas constant | <i>Subscripts</i> | |
| Rc | coating ratio | e | exit |
| t | time, s | in | inlet |
| T | Temperature, K | k | component |

The selectivity of the breakthrough experiments was calculated by

$$Selectivity = \frac{n_i / n_j}{C_i / C_j} \quad (9)$$

6. Crystal Structure Data

Table S1. Crystallographic Data and Structural Refinement Summary for 1.

| | |
|---|--|
| Formula | C ₁₆₂ H ₉₈ O ₅₈ Zn ₉ |
| Fw | 3560.73 |
| <i>T</i> (K) | 293(2) |
| Crystal syst | Cubic |
| space group | <i>P</i> 4(1)32 |
| <i>a</i> (Å) | 26.01190(10) |
| <i>b</i> (Å) | 26.01190(10) |
| <i>c</i> (Å) | 26.01190(10) |
| <i>V</i> (Å ³) | 17600.14(12) |
| α (deg) | 90 |
| β (deg) | 90 |
| γ (deg) | 90 |
| <i>Z</i> | 4 |
| ρ (mg/m ³) | 1.344 |
| θ Range (°) | 3.80-67.09 |
| μ (mm ⁻¹) | 2.020 |
| <i>F</i> (000) | 7216 |
| Range of <i>h, k, l</i> | -30/14,-14/18,-19/30 |
| Total/independent reflections | 11834/5163 |
| Parameters | 362 |
| <i>R</i> indices [<i>I</i> >2 σ (<i>I</i>)] | 0.0760,0.2333 |
| Goodness-of-fit on <i>F</i> ² | 1.057 |
| Residuals (e Å ⁻³) | 1.157/-0.476 |

$$R_1 = \sum ||F_o| - |F_c|| / |F_o|. \quad wR_2 = [\sum w(F_o^2 - F_c^2)^2 / \sum w(F_o^2)^2]^{1/2}.$$

Table S2. Selected bond parameters of compound **1**.

| <i>Bond lengths (Å)</i> | | | |
|----------------------------|----------|---------------------|----------|
| Zn(1)–O(7)#1 | 1.941(6) | Zn(1)–O(5)#2 | 1.947(6) |
| Zn(1)–O(2) | 1.963(6) | Zn(1)–O(1) | 2.024(3) |
| Zn(2)–O(6)#3 | 2.048(6) | Zn(2)–O(3)#5 | 2.075(6) |
| Zn(2)–O(4) | 2.093(6) | | |
| <i>Bond angles (°)</i> | | | |
| O(7)#1–Zn(1)–O(5)#2 | 118.3(3) | O(7)#1–Zn(1)–O(2) | 115.2(3) |
| O(5)#2–Zn(1)–O(2) | 112.6(3) | O(7)#1–Zn(1)–O(1) | 101.9(3) |
| O(5)#2–Zn(1)–O(1) | 102.0(2) | O(2)–Zn(1)–O(1) | 104.1(3) |
| O(6)#3–Zn(2)–O(6)#4 | 96.5(4) | O(6)#3–Zn(2)–O(3)#5 | 82.4(2) |
| O(6)#4–Zn(2)–O(3)#5 | 93.0(3) | O(3)#5–Zn(2)–O(3)#6 | 173.1(4) |
| O(6)#4–Zn(2)–O(4) | 168.8(3) | O(6)#3–Zn(2)–O(4) | 92.4(3) |
| O(3)#6–Zn(2)–O(4) | 90.4(2) | O(3)#5–Zn(2)–O(4) | 94.9(3) |
| O(4)#7–Zn(2)–O(4) | 79.6(3) | | |

Symmetry transformations used to generate equivalent atoms: #1 $x+1/2, -y+3/2, -z+1$; #2 $-x+1/2, -y+1, z+1/2$; #3 $-x, y-1/2, -z+1/2$; #4 $y-3/4, -x+1/4, z-1/4$; #5 $-y+3/4, -x+3/4, -z+3/4$; #6 $-x+1/2, -y+1, z-1/2$.

7. Crystal structure

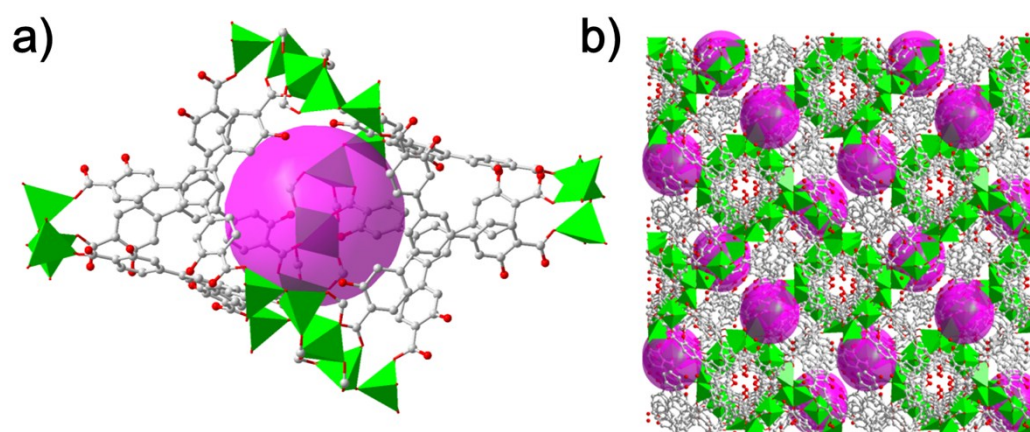


Figure S5. View of (a) the porous trigonal-bipyramid-like polyhedron by six intertwined **L** ligands and metal clusters and (b) 3D porous network.

8. FT-IR spectra

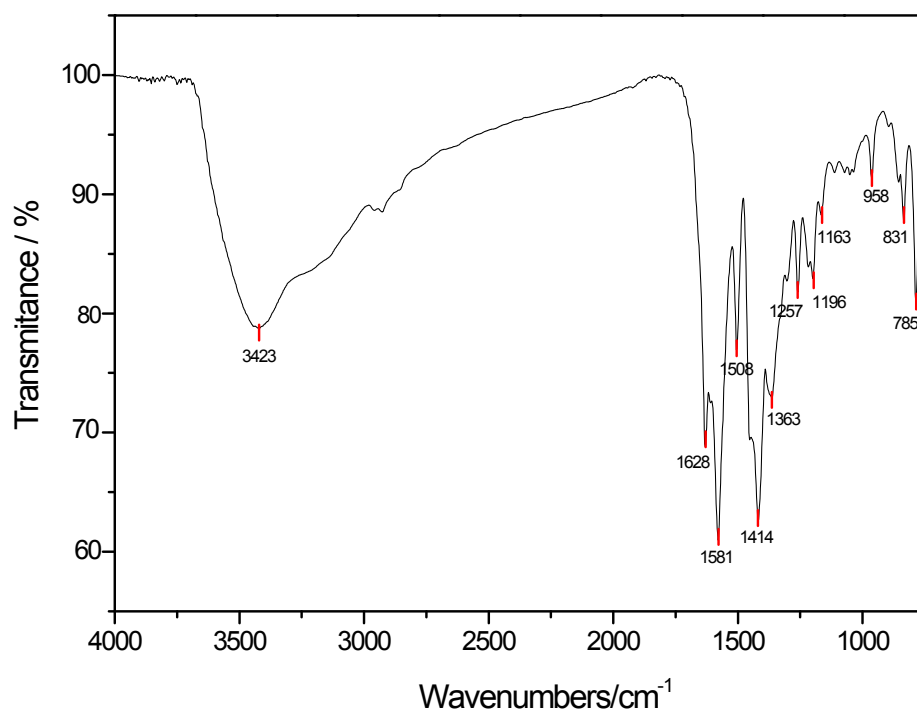


Figure S6. FT-IR spectra for activated **1** (KBr pellet).

9. Thermogravimetric analysis (TGA)

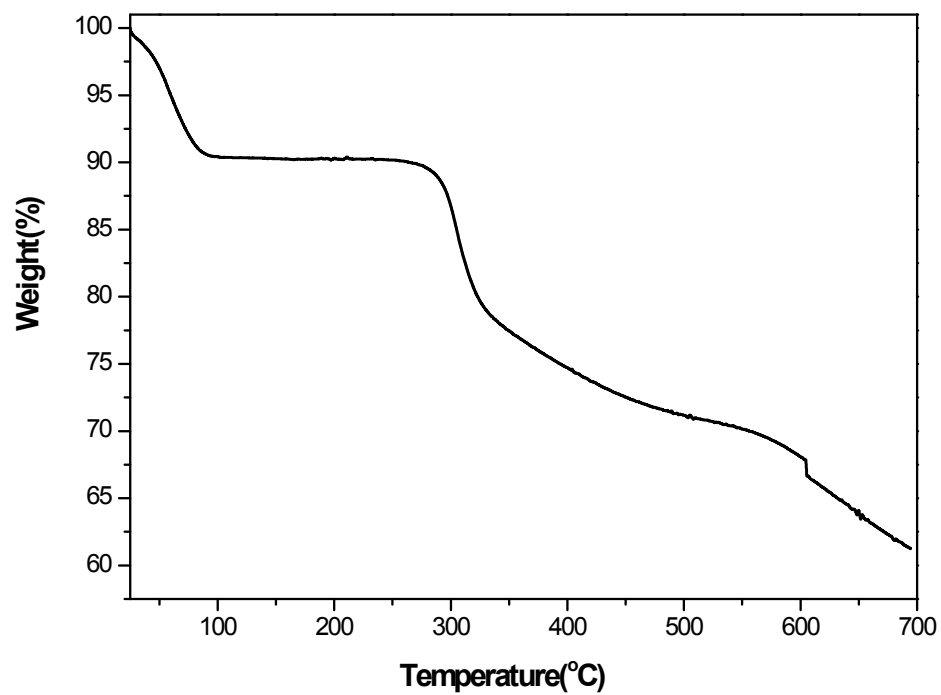


Figure S7. TGA curve of 1.

10. Powder X-Ray Diffraction (PXRD) Characterization

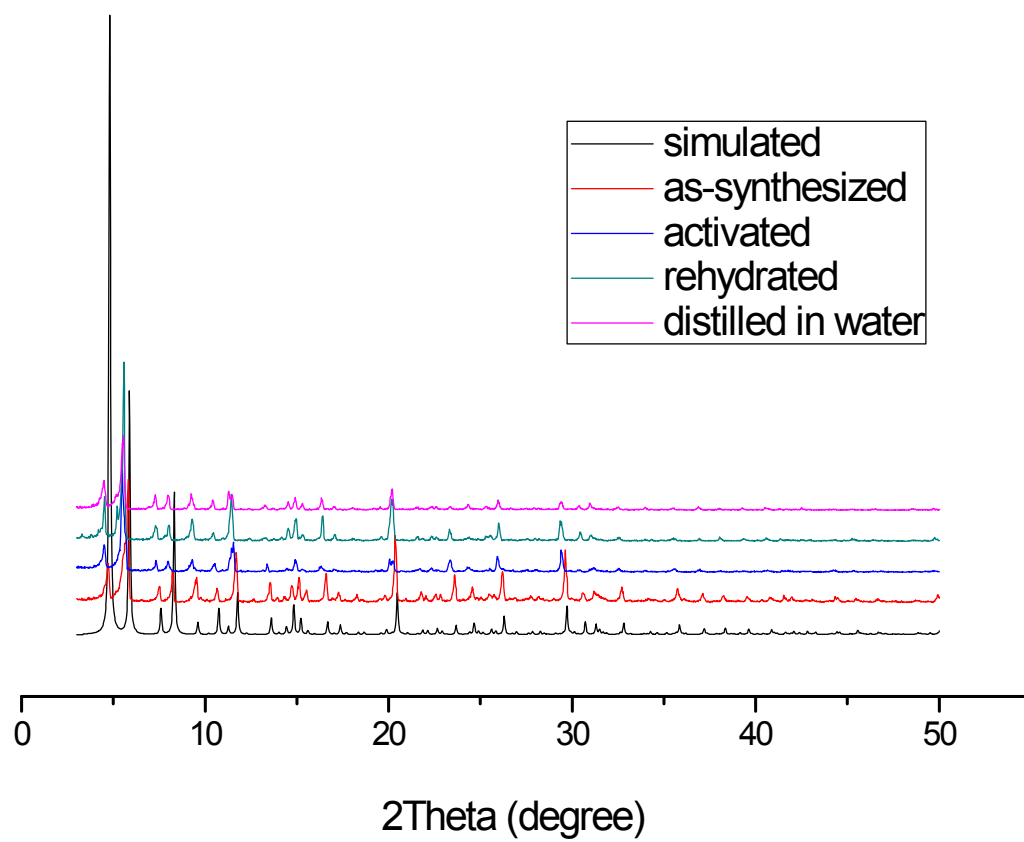


Figure S8. PXRD patterns of **1**.

11. Nitrogen adsorption measurement

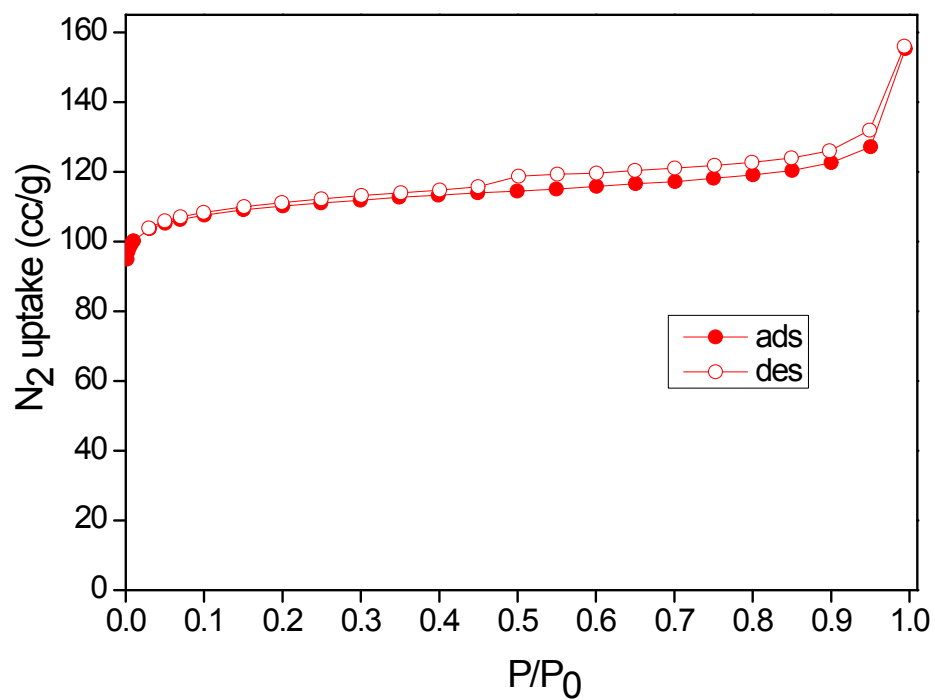


Figure S9. Nitrogen adsorption isotherms of **1**.

12. Molecules distribution in sample 1 upon adsorption

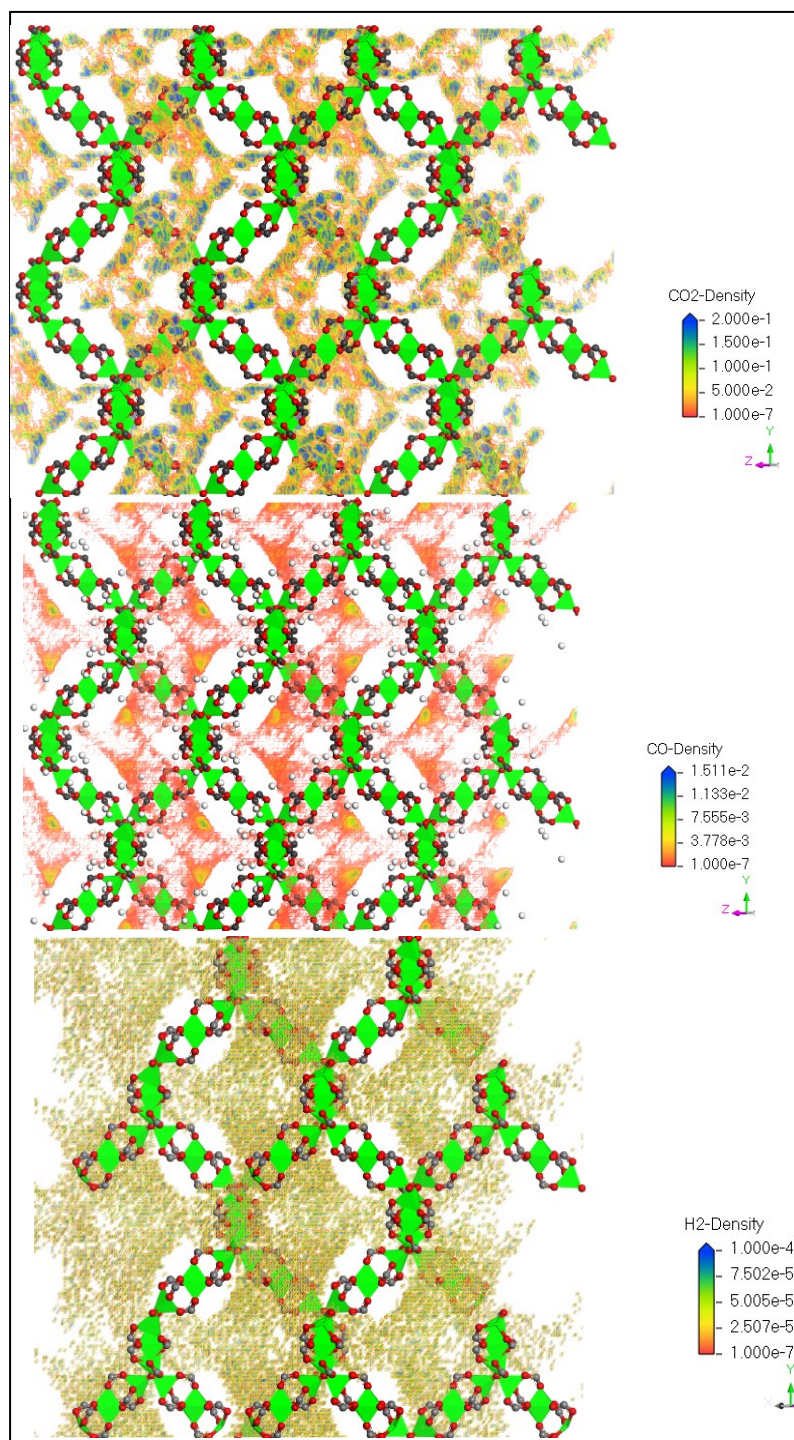


Fig S10. CO₂, CO and H₂ distribution in the sample 1 under 100 kPa at 273 K

13. Isotheric heat of CO₂

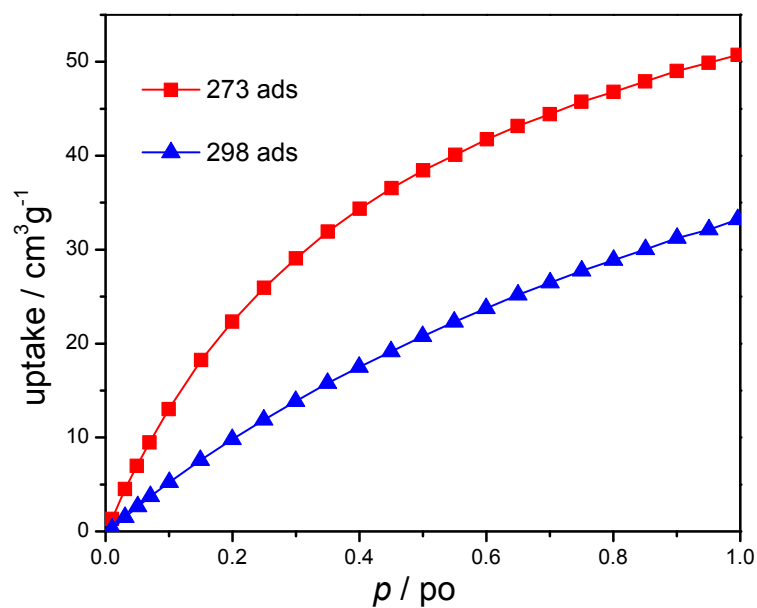


Fig S11. CO₂ isotherm at 273 K(red) and 298K(blue)

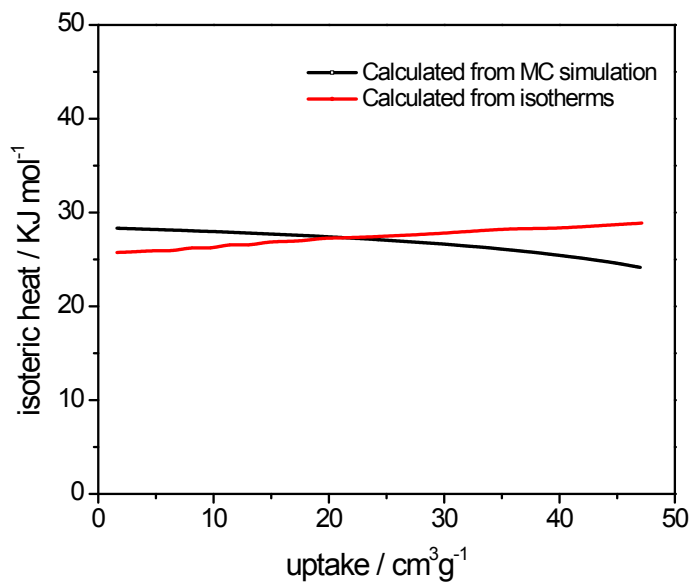


Fig S12. Isotheric heat calculated from MC simulation and isotherms at different temperature according to Clapeyron Equation.

14. Breakthrough experiment

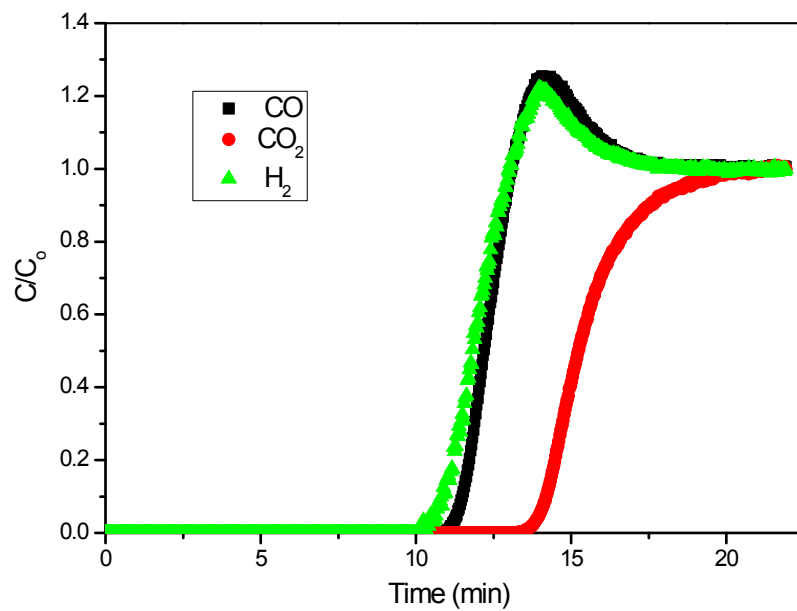


Fig S13. Breakthrough curves of **1** at 273 K and a total mixture gas pressure of 1MPa.